https://doi.org/10.1016/j.jpowsour.2017.07.059

A novel layered perovskite electrode for symmetrical solid oxide fuel cells: $PrBa(Fe_{0.8}Sc_{0.2})_2O_{5+\delta}$

Wei He [b], Xuelian Wu [c], Feifei Dong [a, b, *], Meng Ni [b, **]

[a] *School of Chemical Engineering and Light Industry, Guangdong University of Technology, Guangzhou Higher Education Mega Center, Guangzhou 510006, China*

[b] *Building Energy Research Group, Department of Building and Real Estate, The Hong Kong Polytechnic University, Hung Hom, Kowloon, Hong Kong 999077, China*

[c] *Department of Physics and Materials Science, City University of Hong Kong, Tat Chee Avenue, Kowloon, Hong Kong 999077, China*

[*] Corresponding author.

[**] Corresponding author. Tel.: +852 2766 4152; fax: +852 2764 5131

E-mail addresses: dongff@gdut.edu.cn (F. Dong), meng.ni@polyu.edu.hk (M. Ni)

Abstract

A layered perovskite $PrBa(Fe_{0.8}Sc_{0.2})_2O_{5+\delta}$ (PBFSc) is applied as both cathode and anode in the symmetrical solid oxide fuel cells (SOFCs) field and its electrochemical properties are investigated. $La_{0.9}Sr_{0.1}Ga_{0.8}Mg_{0.2}O_{3-\delta}$ (LSGM) supported symmetrical cell with PBFSc electrode exhibits polarization resistances of 0.05 Ω cm^2 in air and 0.18 Ω cm^2 in wet H_2 at 800 °C. A maximum power density of 921 mW cm^{-2} is obtained using wet H_2 as the fuel and ambient air as the oxidant at 850 °C. Moreover, the electrode demonstrates good redox stability in both oxidizing and reducing atmospheres. The layered perovskite PBFSc with favorable performance characteristics is shown to be an effective, redox-stable electrode candidate that can be used for both cathode and anode.

Keywords: symmetrical solid oxide fuel cell, electrode, layered perovskite, catalytic activity

1. Introduction

Solid oxide fuel cells (SOFCs) are devices that convert chemical energy directly to electric power with high energy conversion efficiency and fuel flexibility [1]. A typical single cell usually consists of three ceramic layers: anode, electrolyte and cathode, and the anode and cathode normally are different components because they are exposed to different atmospheres. Recently, symmetrical SOFCs with a same material as the cathode and anode have attracted much attention [2-4]. This kind of symmetrical configuration leads to a number of advantages, such as decreasing cost for simple fabrication, minimizing compatibility problems, and eliminating possible sulfur poisoning and carbon deposition by simply reversing the gas flows [4].

The requirement for the electrode of symmetrical SOFCs is rather restrictive, because the electrode should be applied in the reducing and oxidizing atmospheres simultaneously as the anode and cathode. It is required that the electrode exhibits robust structural and chemical stability in both reducing and oxidizing environments while maintains sufficient electrical conductivity and electrocatalytic activity [4, 5]. A few materials have been reported as electrodes of symmetrical SOFCs and most of them are perovskite-based oxides. To ensure high stability of electrode, the cations in B-site of those perovskite-based oxides should withstand reduction in reducing environment, therefore, the cations with sufficient chemical stability in reducing atmosphere like Cr, Mo, Nb, Sc and Ti have been doped into B-site of perovskite structure. For instance, $La_{0.75}Sr_{0.25}Cr_{0.5}Mn_{0.5}O_{3-\delta}$, $Sr_2Fe_{1.5}Mo_{0.5}O_{6-\delta}$, $La_{0.4}Sr_{0.6}Co_{0.2}Fe_{0.7}Nb_{0.1}O_{3-\delta}$, $La_{0.8}Sr_{0.2}Sc_{0.2}Mn_{0.8}O_{3-\delta}$ and $La_{0.5}Sr_{0.5}Co_{0.5}Ti_{0.5}O_{3-\delta}$ were

successfully applied in symmetrical SOFCs [2, 6-9]. Additionally, the catalytic activity of fuel oxidation seemed to be improved by doping Sc into perovskite oxides [10].

Recently, layered perovskite oxides have drawn much attention for their significant electronic and electrochemical properties [11-15]. The structure in layered perovskites with ordering of A-site cations localizes the oxygen vacancies within the rare-earth layers and benefits for oxygen ion transfer, which contribute to the rapid surface exchange, bulk diffusion and high catalytic activity [13]. The catalytic activity is mainly affected by the B-site cations [16], and it was reported that some oxides with Fe cations demonstrated high activity for fuel oxidation. For example, $PrBaMn_{1.5}Fe_{0.5}O_{5+\delta}$ and $(PrBa)_{0.95}(Fe_{0.9}Mo_{0.1})_2O_{5+\delta}$ have been reported as potential electrodes in symmetrical SOFCs, which both exhibited excellent stability and good catalytic activity under reducing atmosphere [5, 17].

Herein, the iron-rich layered perovskite $PrBa(Fe_{0.8}Sc_{0.2})_2O_{5+\delta}$ (PBFSc) was applied as the electrode of symmetrical SOFCs and the electrochemical properties were investigated. The layered perovskite demonstrated high electrocatlytic activity in both oxidizing and reducing atmospheres and good redox stability, indicating a promising electrode for symmetrical SOFCs.

2. Experimental

2.1. Powder synthesis: PBFSc powder was synthesized by a sol-gel combustion method. The metal nitrates of $Ba(NO_3)_2$, $Pr(NO_3)_3{\cdot}6H_2O$, $Fe(NO_3)_3{\cdot}9H_2O$ and $Sc(NO_3)_3$ ($Sc(NO_3)_3$ was prepared by dissolving Sc_2O_3 powder in nitric acid) with stoichiometric ratio were dissolved in deionized water. The ethylenediaminetetraacetic acid (EDTA) and

citric acid were added into the solution as complexing agents, and extra acid was neutralized by $NH_3 \cdot H_2O$ to keep pH ~7. After heating with stirring, a gel was obtained. This gel was fired at 250 °C to form a precursor, and subsequently calcined at 1100 °C for 2 h to obtain the PBFSc powder. The LSGM was synthesized by a solid-state reaction method [18].

2.2. Cell fabrication: Symmetrical cells with PBFSc|LSGM|PBFSc configuration were fabricated by spraying PBFSc slurries on the surface of the dense LSGM pellets. The dense LSGM substrates were prepared by dry pressing method with subsequent calcination at 1450 °C for 5 h. The PBFSc slurries were prepared by dispersing powder in mixed solution of glycerol, ethylene glycol, and isopropyl alcohol via ball-milling. After spraying the electrode, the cells were finally calcined at 900 °C for 0.5 h in air.

2.3. Characterization: The crystal structure of the PBFSc powder was characterized by X-ray diffraction (XRD, Rigaku Smartlab) and transmission electron microscope (TEM, JEOL JEM-2100F) equipped with energy dispersive X-ray (EDX). The XRD pattern was further refined by Fullprof [19]. The microstructures of the cell were observed by scanning electron microscope (SEM, JEOL 6490). For the electrical conductivity, the bar-shaped dense samples were preferred and tested by a four-probe DC method with a Keithley 2420 source meter. The impedance spectra of the symmetrical cell were measured using a Solartron 1260A frequency response analyzer with a Solartron 1287 potentiostat with frequency from 0.1 Hz to 1 MHz at open circuit condition (AC amplitude 10 mV). Performances of single cells were investigated by a homemade testing system and *I-V* curves were also obtained by a Keithley 2420 digital source meter using four probe configuration.

3. Results and discussion

Fig. 1a presents the refined XRD pattern of PBFSc. The PBFSc powder exhibits a well-formed tetragonal structure with space group of P4/mmm. The lattice parameter of a = b is calculated to be ~3.95 Å, which is approximately half of parameter c (7.91 Å) due to the ordered Pr and Ba cations. The low reliability factors of R_p = 6.83%, R_{wp} = 9.03%, and χ^2 = 1.60 imply the validity of refinement result. The PBFSc powder is further investigated by the TEM. Fig. 1b shows that PBFSc sample displays well-defined lattice fringes in the high-resolution TEM image. The crystal structure is also confirmed by the corresponding fast Fourier transform (FFT) pattern along the [0 $\overline{2}$ 1] zone axis (Fig. 1c). An interplanar spacing of 3.94 Å, which is related to (100) lattice plane, is obtained in reverse FFT from Fig. 1d. The TEM analysis is in agreement with the Rietveld refinement result of XRD pattern (d_{100} = 3.95 Å). The Pr, Ba, Fe, and Sc elements are detected by the EDX spectroscopy as shown in Fig. S1. The results above suggest that the Sc has been incorporated into the layered perovskite PBFSc. In addition, the structure of the PBFSc in reducing atmosphere is investigated, with the results shown in Fig. S2. After annealing in 5% H_2/N_2 and wet H_2 for 10 h at 800 °C respectively, the phase structure of PBFSc powder is retained, indicating the superior structural stability of PBFSc in reducing atmosphere.

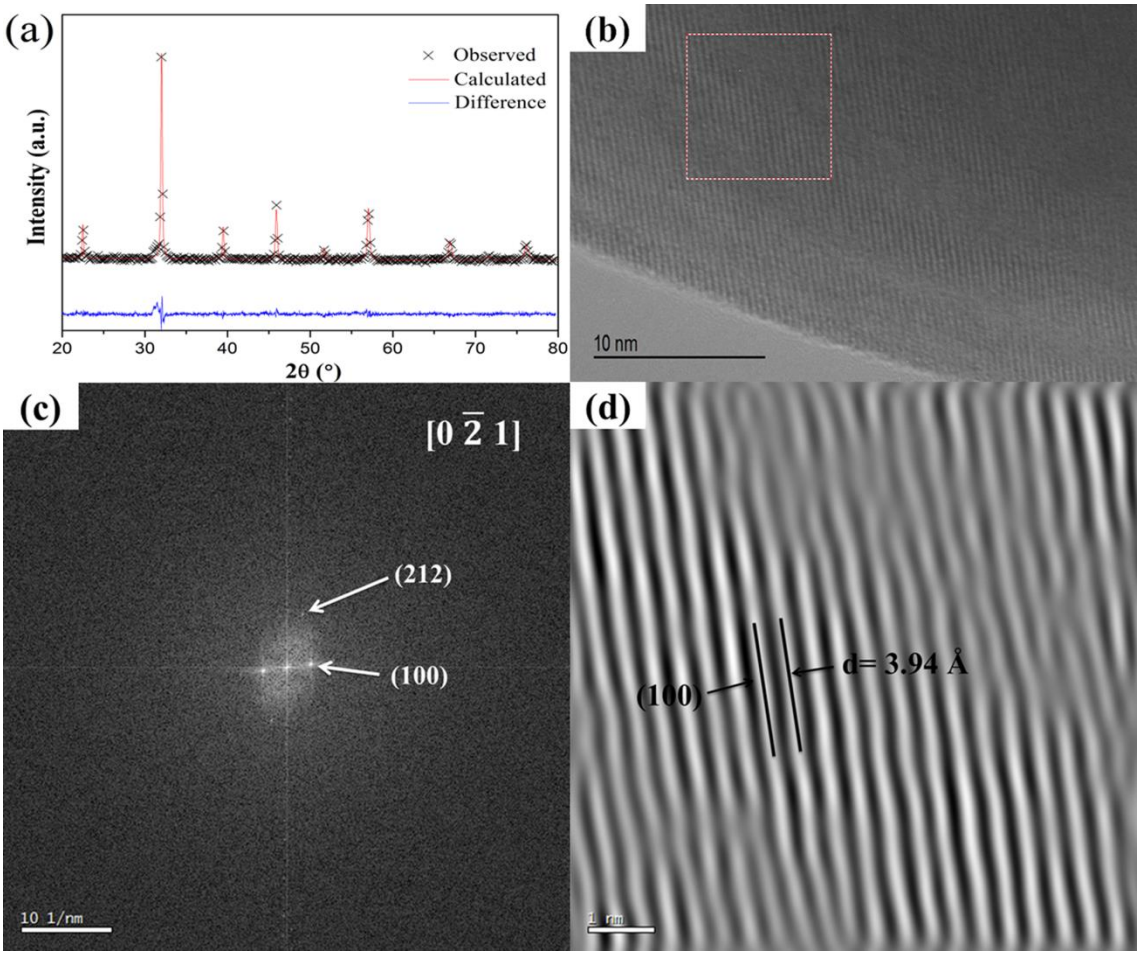

Fig. 1. (a) XRD pattern of PBFSc, (b) high-solution TEM image of PBFSc, (c) FFT pattern of the selected region, (d) reverse FFT image of the selected region.

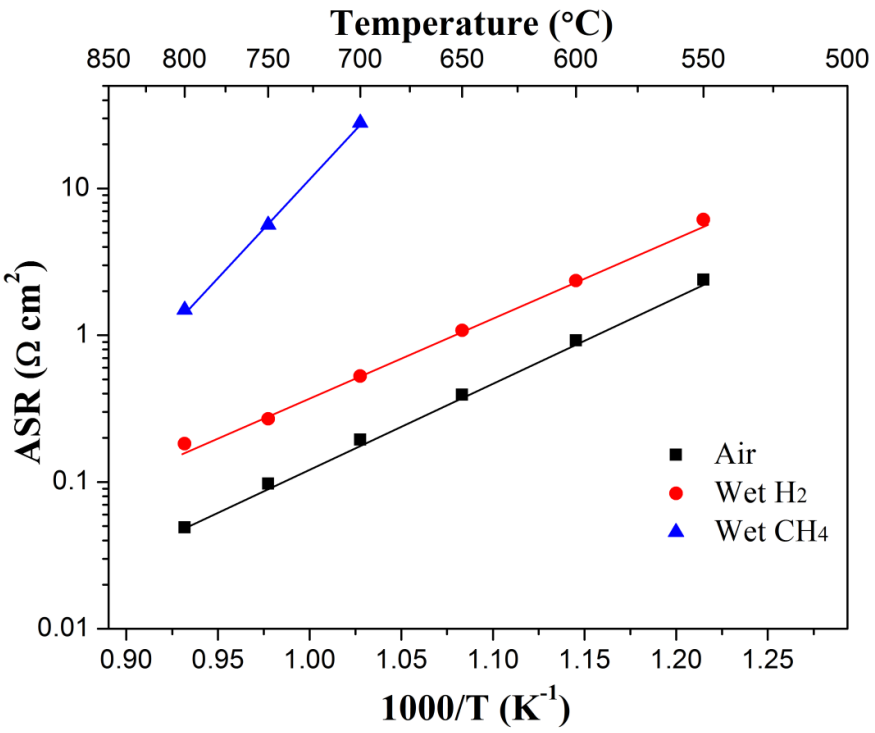

Fig. 2. Arrhenius plots of ASR values of PBFSc electrode in air, wet H_2 and wet CH_4.

Fig. S3 shows the electrical conductivities of the PBFSc versus temperature in air, 5% H_2 and wet H_2. The electrical conductivities are not high but achieve the minimum required value of 0.01 S cm^{-1} [20], and values in reducing atmospheres are comparable to those of $La_{0.75}Sr_{0.25}Cr_{0.5}Mn_{0.5}O_{3-\delta}$ electrode under similar condition [21]. The lower conductivity in more reducing atmosphere may be ascribed to the loss of the electron holes after thermal reduction [5]. The electrochemical properties are evaluated by area specific resistances (ASRs) in different gas conditions, which are measured by electrochemical impedance spectroscopy (EIS) for the PBFSc|LSGM|PBFSc symmetrical cell configuration, and the results are shown in Fig. 2. The ASRs in air are 0.05, 0.19 and 0.92 Ω cm^2 at 800, 700 and 600 °C, respectively, which are lower than those of some prevailing cathode materials deposited on the same electrolyte, such as $La_{0.9}Sr_{0.1}MnO_{3-\delta}$ (~10 Ω cm^2 at 870 °C) [22],

$La_{0.6}Sr_{0.4}Co_{0.8}Fe_{0.2}O_{3-\delta}$ (0.28 Ω cm^2 at 800°C) [23], and $Sm_{0.5}Sr_{0.5}CoO_{3-\delta}$ (0.45 Ω cm^2 at 800 °C) [24]. The PBFSc also exhibits excellent catalytic activity in humidified H_2 (3% H_2O). The ASRs of 0.18, 0.53 and 2.35 Ω cm^2 are observed at 800, 700 and 600 °C, respectively, which are similar to those of some perovskite-based anode materials, e.g. $La_{0.75}Sr_{0.25}Cr_{0.5}Mn_{0.5}O_{3-\delta}$ (0.3 Ω cm^2 at 900 °C in wet H_2) [2], $Sr_2Fe_{1.5}Mo_{0.5}O_{6-\delta}$ (0.27 Ω cm^2 at 800 °C in wet H_2) [6], and $PrBaMn_{1.5}Fe_{0.5}O_{5+\delta}$ (0.68 Ω cm^2 at 800 °C in 5% H_2) [5]. The ASRs of PBFSc increase to 1.49 and 5.65 Ω cm^2 at 800 and 750 °C, respectively, while the atmosphere is switched to humidified CH_4.

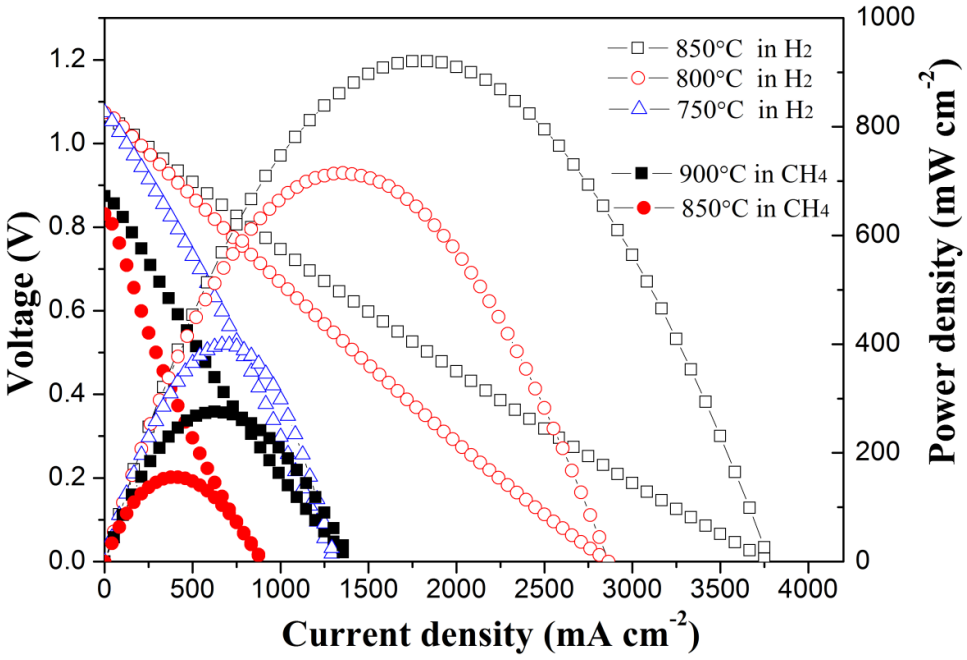

Fig. 3. *I-V* curves and corresponding power densities of a symmetrical cell with PBFSc electrode using wet H_2 and wet CH_4 as the fuels at different temperatures.

Fig. 3 presents the electrochemical performance of electrolyte-supported symmetrical cell with PBFSc electrode measured using two different fuels. The thickness of dense

LSGM electrolyte is approximately 275 μm, as shown in Fig. S4. In the case of wet H_2 as the fuel, the open circuit voltages (OCVs) of cell are all above 1.067 V from 750 to 850 °C, which are close to the theoretical values. The maximum power densities of 921, 713 and 398 mW cm^{-2} are observed at 850, 800 and 750 °C, respectively, which are higher than those obtained for similar cell configuration by applying other symmetrical electrodes like $Sr_2Fe_{1.5}Mo_{0.5}O_{6-\delta}$, $La_{0.5}Sr_{0.5}Co_{0.5}Ti_{0.5}O_{3-\delta}$, and $La_{0.7}Ca_{0.3}CrO_3$–$Ce_{0.8}Gd_{0.2}O_{1.9}$ [6, 9, 25]. The high performance may be ascribed to its low resistances, which are shown in Fig. S5a. The internal polarization resistances under open circuit condition (difference between high and low frequency intercept on the real axis) are 0.19, 0.28 and 0.39 Ω cm^2 at 850, 800 and 750 °C, respectively. The ohmic resistances (high frequency intercept, mainly electrolyte resistances) can't be ignored, indicating that reducing the electrolyte thickness will decrease the whole resistance and improve the performance. The performance and impedance spectra of the cell using wet CH_4 as the fuel are presented in Fig. 3 and Fig. S5b. The cell performance is lower than that in H_2 condition. A maximum power density of 275 mW cm^{-2} is obtained at 900 °C, which is comparable to that of $Sr_2Fe_{1.5}Mo_{0.5}O_{6-\delta}$ electrode. It is noted that OCVs in wet CH_4 are lower than the calculated theoretical potentials. This phenomenon is mostly due to the low conversion of methane in the anode side [26]. The catalytic activity of electrode for CH_4 oxidation is not as good as that for H_2 oxidation, some researches revealed that impregnation or doping of Ni could improve the cell performance in CH_4 [27-29].

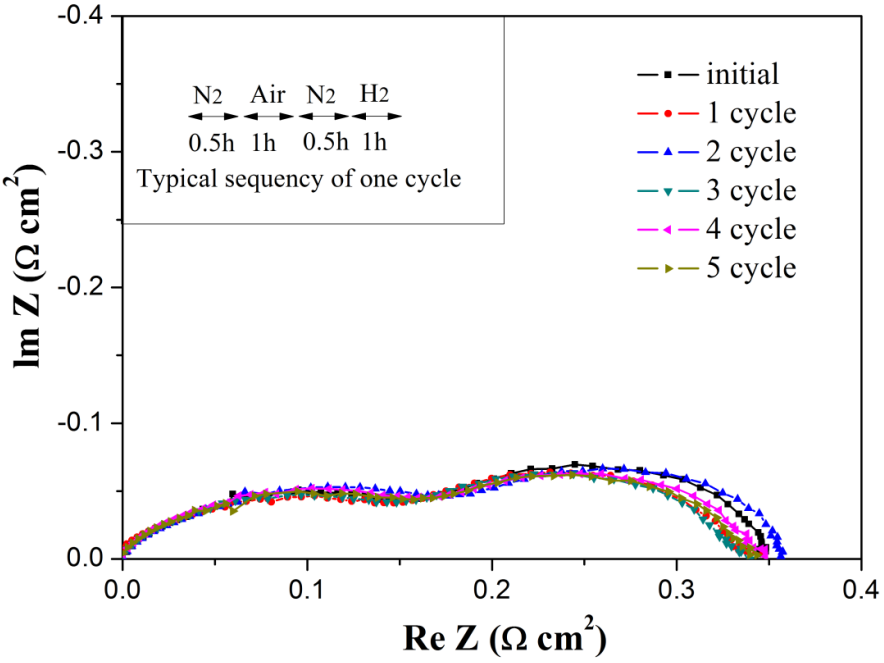

Fig. 4. Polarization impedance of single cell at 750 °C after each cycling test.

Redox stability is of importance for electrode in symmetrical SOFCs for its unique operating conditions. The stability is measured by a symmetrical cell using the wet H_2 as the fuel and the ambient air as the oxidant at 750 °C. The anode gas is switched between the wet H_2 and the air. In one cycle, electrode is oxidized and reduced by air and wet H_2 respectively, and the N_2 serves as the protection gas. After each redox cycle, the impedance spectra of electrode in wet H_2 are shown in Fig. 4 under open circuit condition. The interfacial polarization resistances are around 0.35 Ω cm^2 in the redox test, indicating the good redox stability of the electrode.

4. Conclusions

In summary, layered perovskite PBFSc was synthesized and its properties were investigated. The PBFSc demonstrated high catalytic activity and redox stability in oxidizing and reducing atmospheres. With these particular properties, a symmetrical SOFC with PBFSc electrode as both cathode and anode was fabricated and a favorable electrochemical performance was achieved. The superior electrocatalytic performance justifies the potential of PBFSs as an electrode for symmetrical SOFCs.

Acknowledgements

This work was supported by a grant (Project Number: PolyU 152127/14E) from Research Grant Council, University Grants Committee, Hong Kong SAR; a grant from The Hong Kong Polytechnic University (Account: 1-ZVFQ); a startup R&D funding from One-Hundred Young Talents Program of Guangdong University of Technology (No.: 220413180).

Appendix A. Supplementary data

Supplementary data related to this article can be found at

References

[1] N. Mahato, A. Banerjee, A. Gupta, S. Omar, K. Balani, Prog. Mater. Sci. 72 (2015) 141-337.

[2] D.M. Bastidas, S.W. Tao, J.T.S. Irvine, J. Mater. Chem. 16 (2006) 1603-1605.

[3] C. Su, W. Wang, M. Liu, M.O. Tadé, Z. Shao, Adv. Energy Mater. 5 (2015) 1500188.

[4] J.C. Ruiz-Morales, D. Marrero-Lopez, J. Canales-Vazquez, J.T.S. Irvine, RSC Adv. 1 (2011) 1403-1414.

[5] L. Zhao, K. Chen, Y. Liu, B. He, J. Power Sources 342 (2017) 313-319.

[6] Q. Liu, X. Dong, G. Xiao, F. Zhao, F. Chen, Adv. Mater. 22 (2010) 5478-5482.

[7] Z. Yang, N. Xu, M. Han, F. Chen, Int. J. Hydrogen Energy 39 (2014) 7402-7406.

[8] Y. Zheng, C. Zhang, R. Ran, R. Cai, Z. Shao, D. Farrusseng, Acta Mater. 57 (2009) 1165-1175.

[9] R. Martinez-Coronado, A. Aguadero, D. Perez-Coll, L. Troncoso, J.A. Alonso, M.T. Fernandez-Diaz, Int. J. Hydrogen Energy 37 (2012) 18310-18318.

[10] J. Canales-Vazquez, J.C. Ruiz-Morales, J.T.S. Irvine, W. Zhou, J. Electrochem. Soc. 152 (2005) A1458-A1465.

[11] K. Zhang, L. Ge, R. Ran, Z. Shao, S. Liu, Acta Mater. 56 (2008) 4876-4889.

[12] S. Sengodan, S. Choi, A. Jun, T.H. Shin, Y.W. Ju, H.Y. Jeong, J. Shin, J.T.S. Irvine, G. Kim, Nat. Mater. 14 (2015) 205-209.

[13] G. Kim, S. Wang, A.J. Jacobson, L. Reimus, P. Brodersen, C.A. Mims, J. Mater. Chem. 17 (2007) 2500-2505.

[14] Y.H. Huang, G. Liang, M. Croft, M. Lehtimäki, M. Karppinen, J.B. Goodenough, Chem. Mater. 21 (2009) 2319-2326.

[15] F. Dong, M. Ni, Y. Chen, D. Chen, M.O. Tadé, Z. Shao, J. Mater. Chem. A 2 (2014) 20520-20529.

[16] F. Dong, M. Ni, W. He, Y. Chen, G. Yang, D. Chen, Z. Shao, J. Power Sources 326 (2016) 459-465.

[17] H. Ding, Z. Tao, S. Liu, J. Zhang, Sci. Rep. 5 (2015) 18129.

[18] N. Trofimenko, H. Ullmann, Solid State Ionics 124 (1999) 263-270.

[19] J. Rodriguez-Carvajal, Physica B 192 (1993) 55-69.

[20] M.D. Gross, J.M. Vohs, R.J. Gorte, Electrochem. Solid-State Lett. 10 (2007) B65-B69.

[21] S. Tao, J.T.S. Irvine, J. Electrochem. Soc. 151 (2004) A252-A259.

[22] S. Wang, X. Lu, M. Liu, J. Solid State Electrochem. 6 (2002) 384-390.

[23] W. Guo, J. Liu, C. Jin, H. Gao, Y. Zhang, J. Alloy Compd. 473 (2009) 43-47.

[24] L. Fan, Y. Wang, Z. Jia, Y. Xiong, M.E. Brito, Ceram. Int. 41 (2015) 6583-6588.

[25] Y. Zhang, Q. Zhou, T. He, J. Power Sources 196 (2011) 76-83.

[26] S.P. Jiang, X.J. Chen, S.H. Chan, J.T. Kwok, K.A. Khor, Solid State Ionics 177 (2006) 149-157.

[27] X. Zhu, Z. Lü, B. Wei, X. Huang, Y. Zhang, W. Su, J. Power Sources 196 (2011) 729-733.

[28] Z. Du, H. Zhao, S. Yi, Q. Xia, Y. Gong, Y. Zhang, X. Cheng, Y. Li, L. Gu, K. Swierczek, ACS Nano 10 (2016) 8660-8669.

[29] G. Yang, C. Su, R. Ran, M.O. Tadé, Z. Shao, Energy Fuels 28 (2014) 356-362.

Figure Captions

Fig. 1. (a) XRD pattern of PBFSc, (b) high-solution TEM image of PBFSc, (c) FFT pattern of the selected region, (d) reverse FFT image of the selected region.

Fig. 2. Arrhenius plots of ASR values of PBFSc electrode in air, wet H_2 and wet CH_4.

Fig. 3. *I-V* curves and corresponding power densities of a symmetrical cell with PBFSc electrode using wet H_2 and wet CH_4 as the fuels at different temperatures.

Fig. 4. Polarization impedance of single cell at 750 °C after each cycling test.

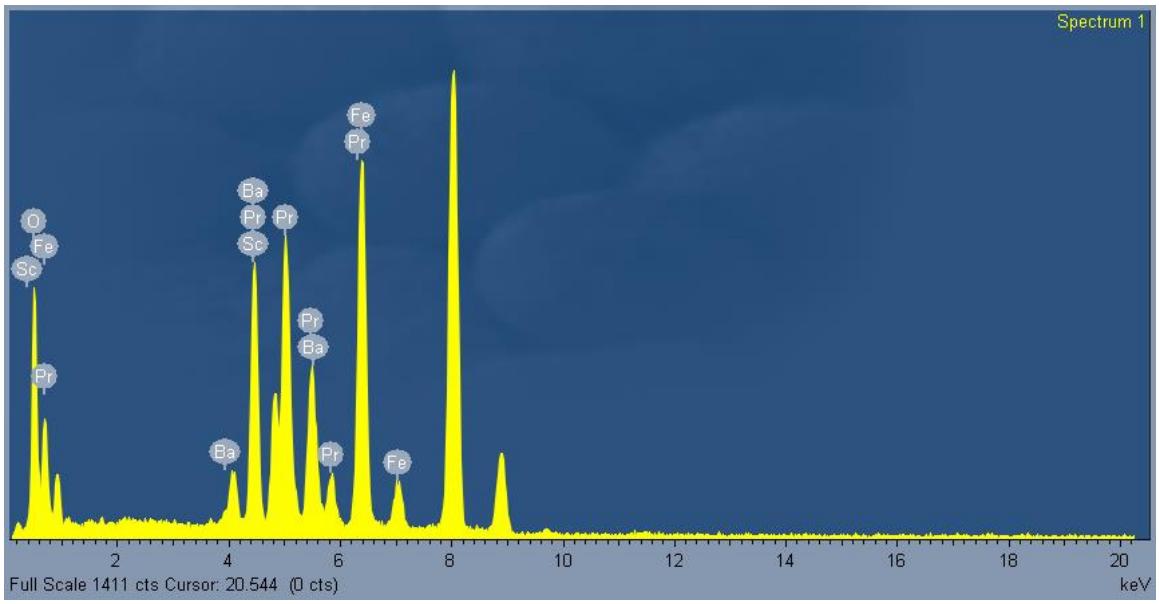

Fig. S1. EDX spectroscopy of PBFSc powder.

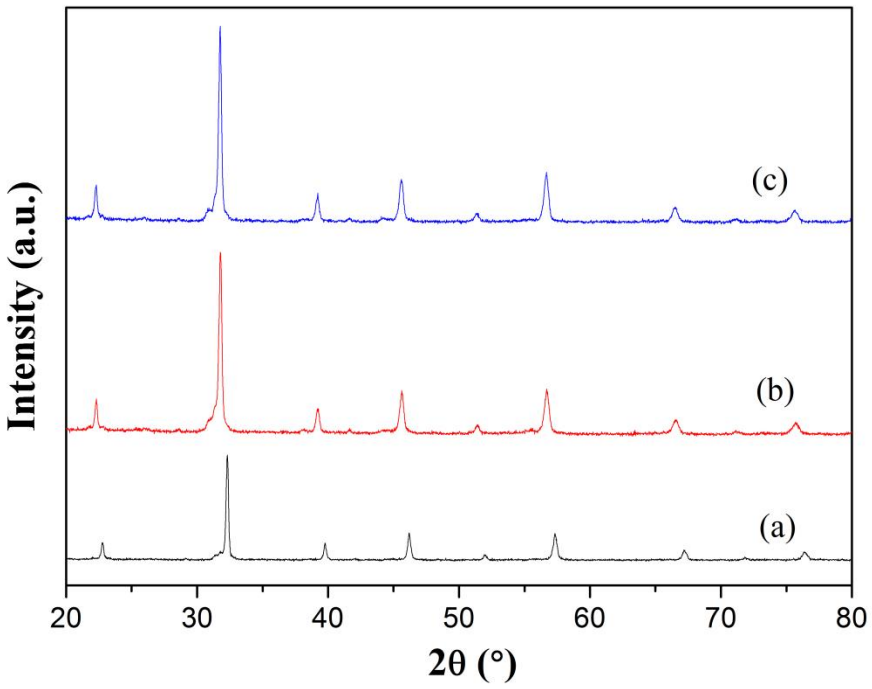

Fig. S2. XRD patterns of PBFSc powder (a) as-prepared, (b) after thermal treatment in 5% H_2 for 10 h, (c) after thermal treatment in wet H_2 for 10 h.

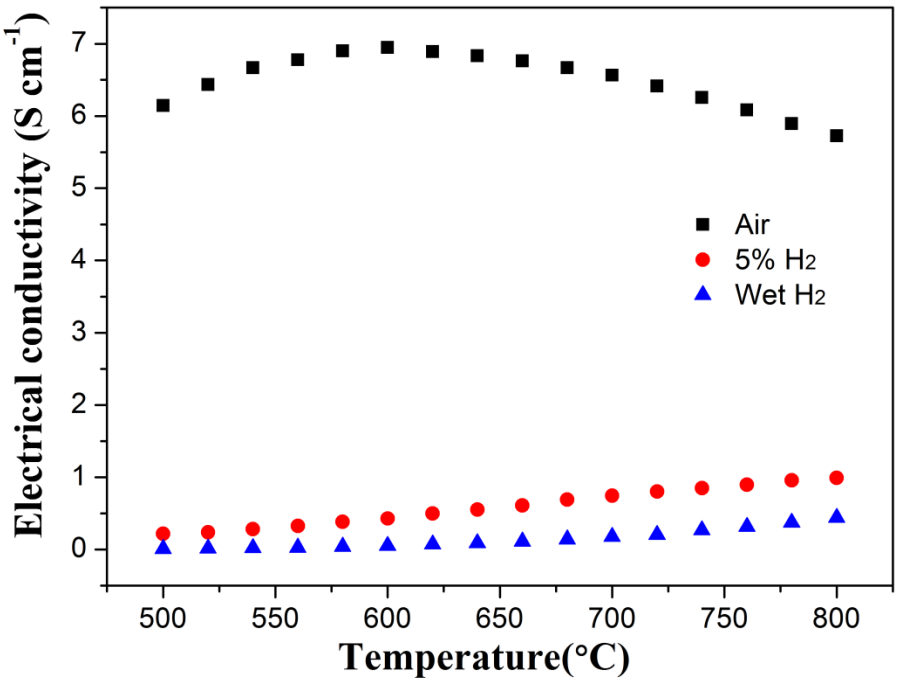

Fig. S3. Electrical conductivities of PBFSc in air, 5% H_2 and wet H_2.

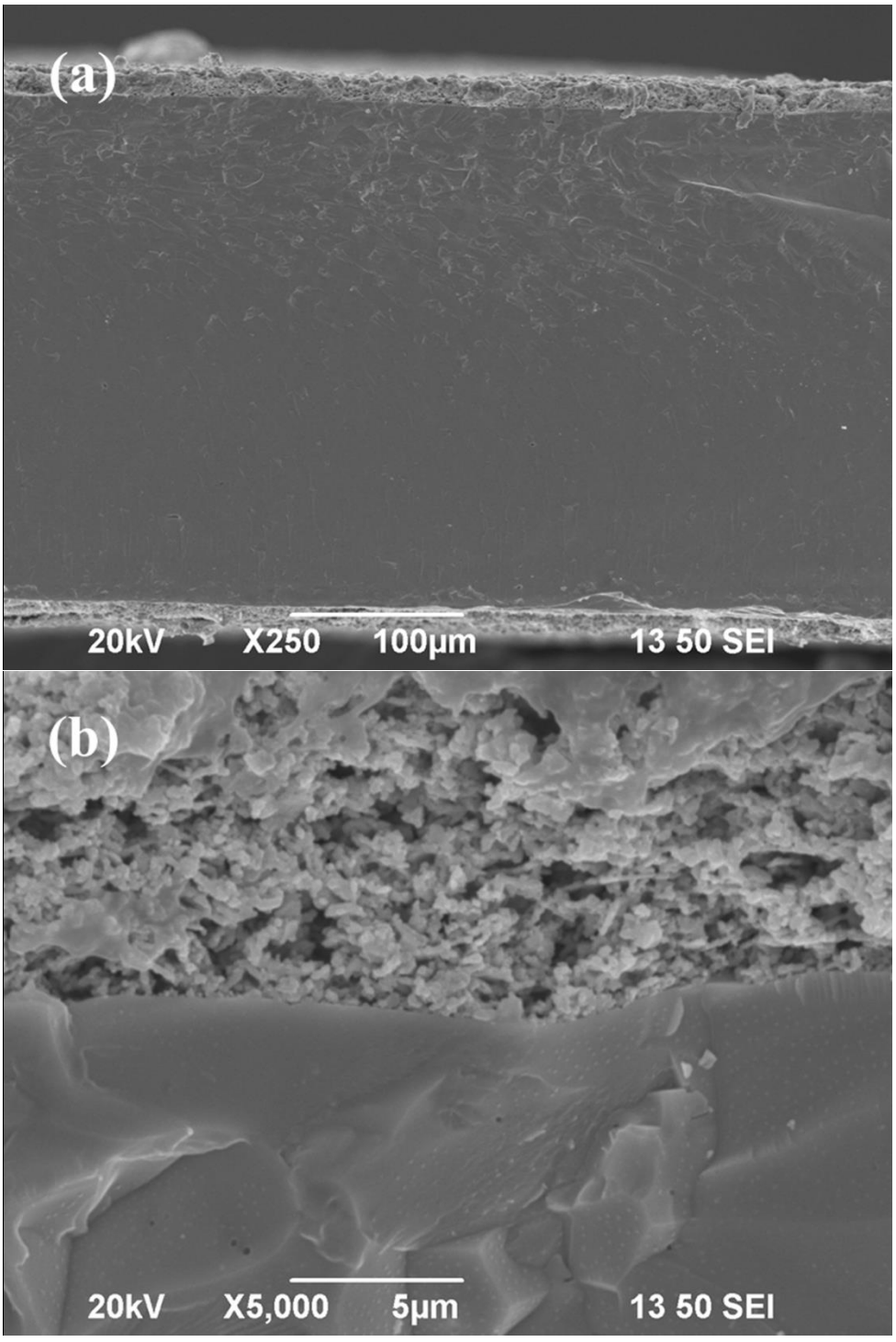

Fig. S4. (a) Cross-sectional SEM image of a symmetrical cell with PBFSc electrode, (b) close-up image of the interface between electrode and electrolyte.

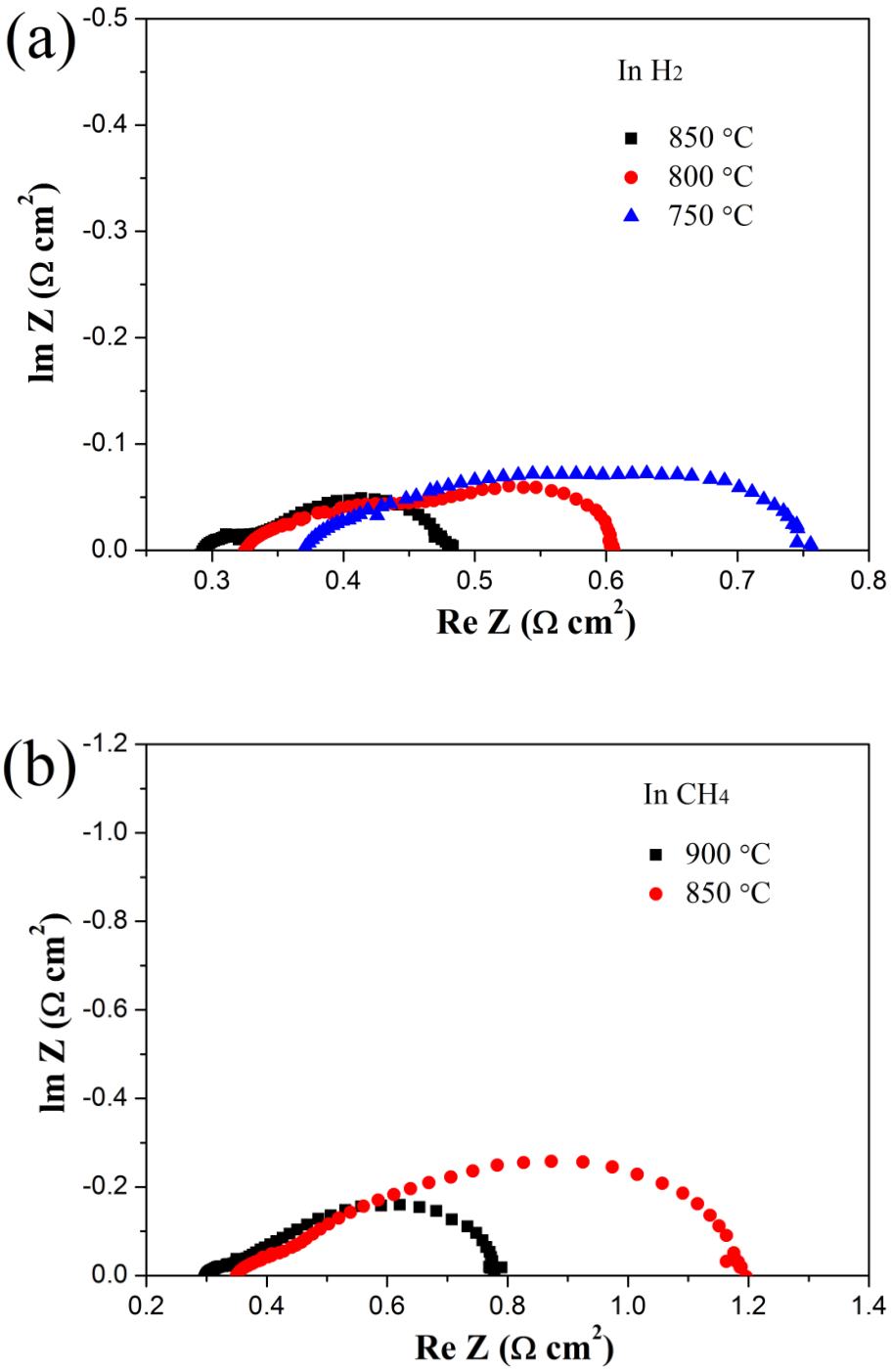

Fig. S5. Impedance spectra of symmetrical cells measured under open-circuit conditions using different fuels (a) wet H_2 as the fuel, (b) wet CH_4 as the fuel.